Electronic Supplementary Material (ESI) for Journal of Materials Chemistry A.

Supporting information for

Surface etching of HKUST-1 promoted via supramolecular interactions for chromatography

Samir El-Hankari, Jia Huo, Adam Ahmed, Haifei Zhang and Darren Bradshaw*

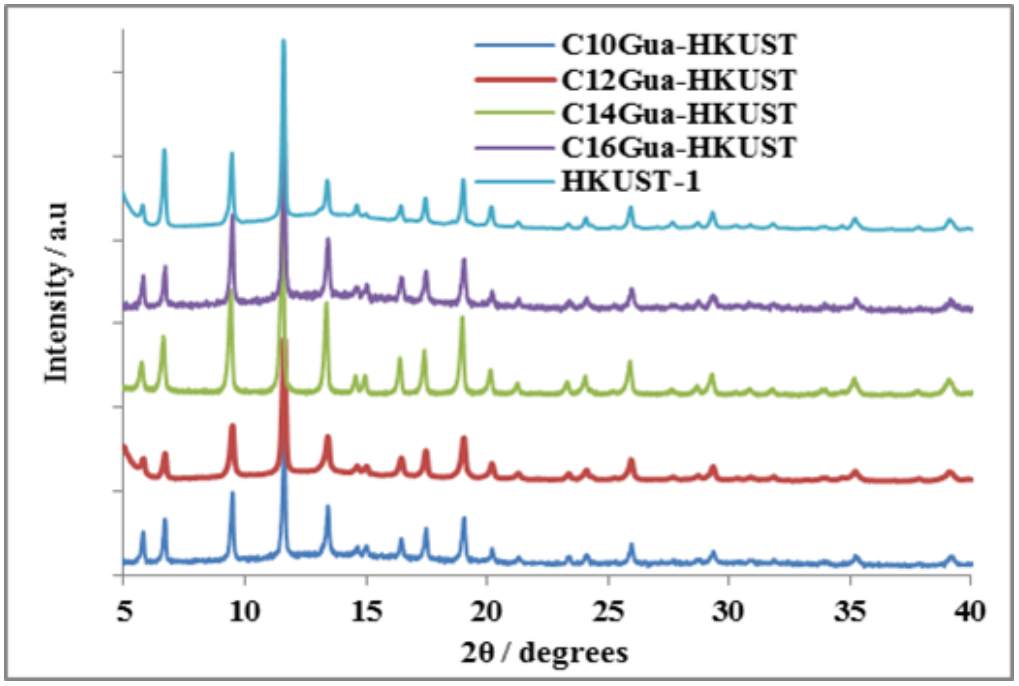

Figure S1. PXRD data of C_nGua-HKUST-1 materials prepared in the presence of C_nGua surfactants compared to a pure bulk sample of HKUST-1

Material	Micropore uptake[a] / cm^3g^{-1}	S_{BET} /m^2g^{-1}	Average pore diameter[b] / nm
C_{10}Gua-HKUST-1	195	739	56
C_{12}Gua-HKUST-1	167	653	73
C_{14}Gua-HKUST-1	149	581	53
C_{16}Gua-HKUST-1	127	489	68
HKUST-1	271	1069	-

[a] Determined at $p/p^0 = 0.3$; [b] Estimated at the maximum of the BJH pore size distribution.

Table S1. Porosity data and surface properties of the C_nGua-HKUST-1 phases determined from the N_2 adsorption isotherms shown in manuscript figure 2.

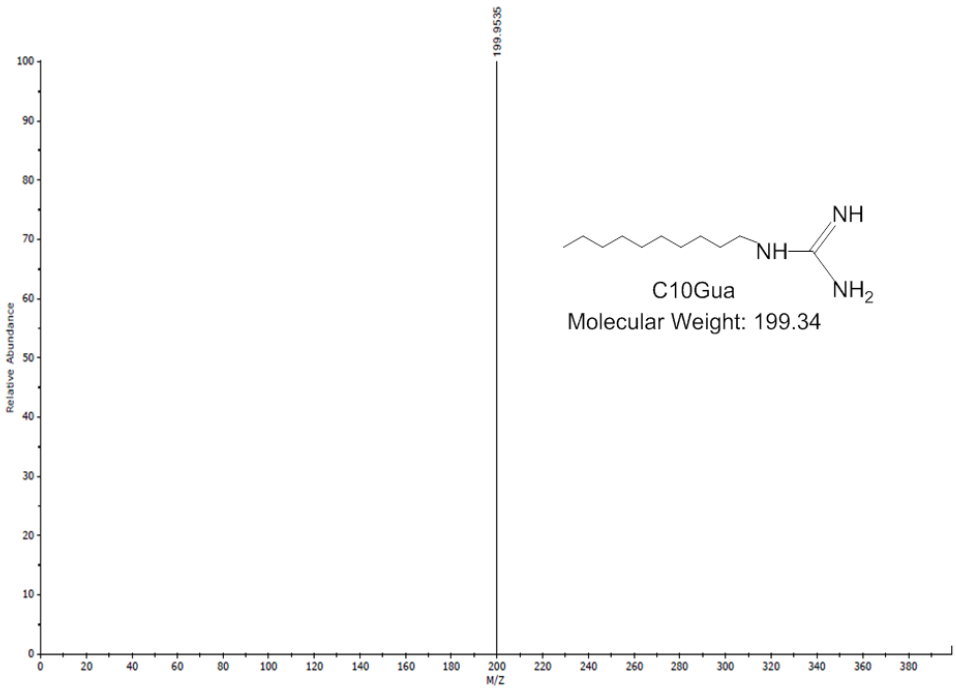
199.9535
Relative Abundance
M/Z
NH
NH
NH2
C10Gua
Molecular Weight: 199.34

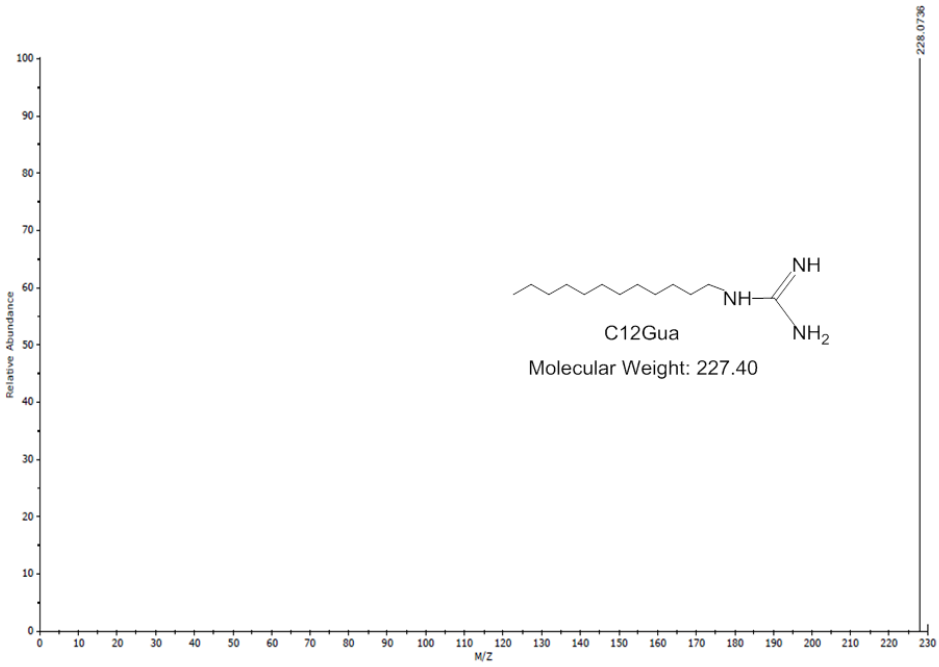
228.0736
Relative Abundance
M/Z
NH
NH
NH2
C12Gua
Molecular Weight: 227.40

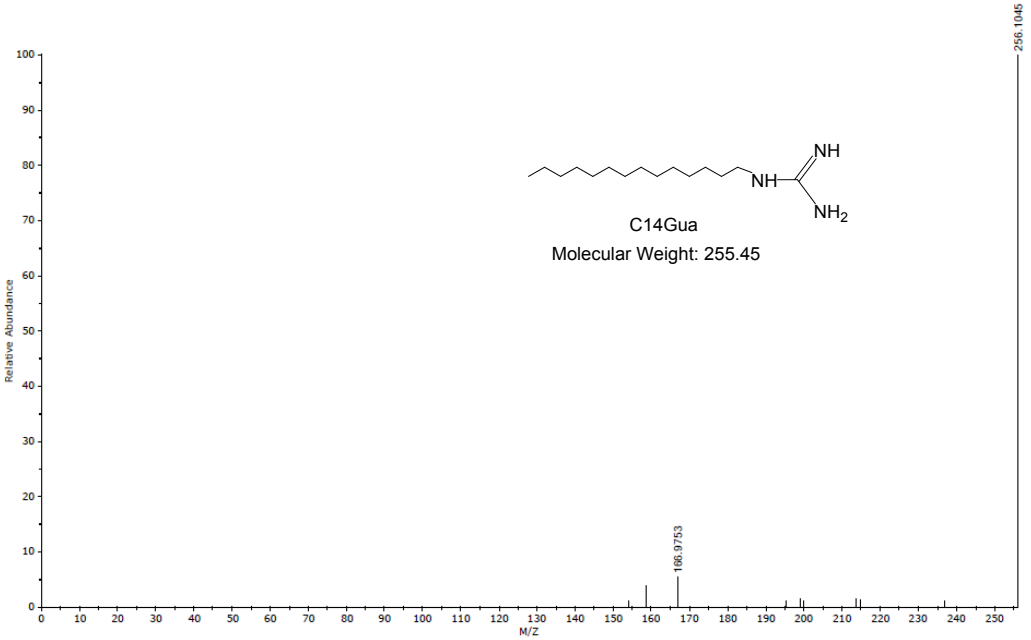

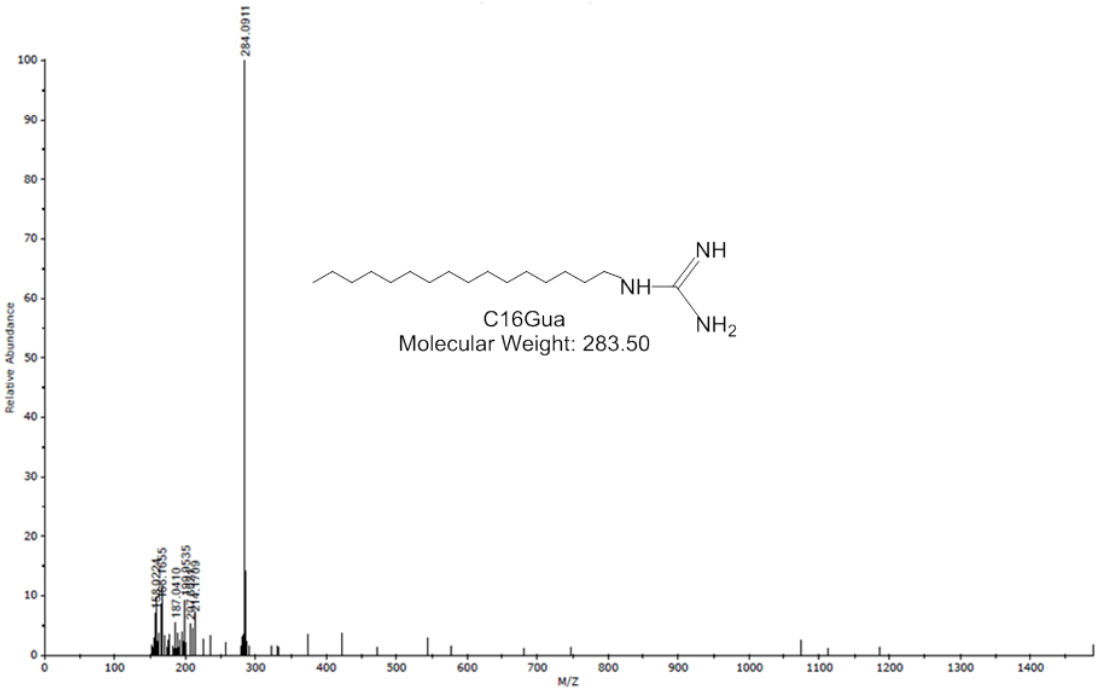

Figure S2. ES-MS data of C_nGua-HKUST-1 following acid digestion and filtration, which clearly identifies the presence of residual C_nGua species in all cases.

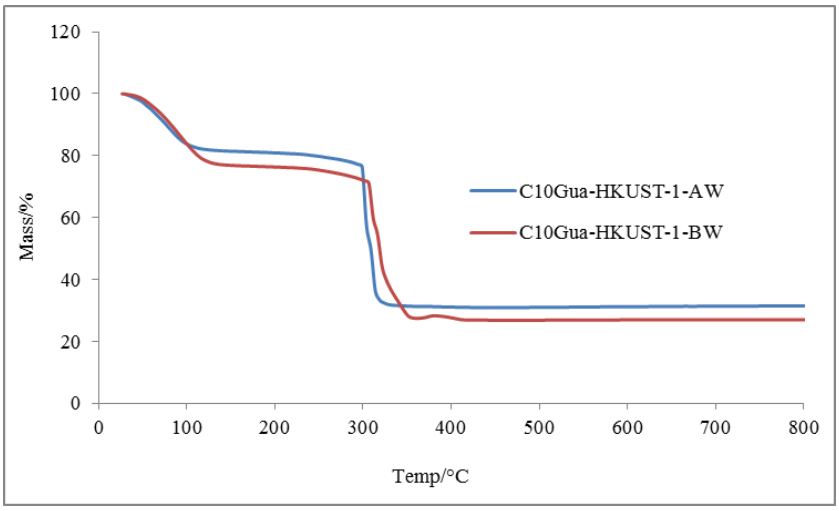

Figure S3. TGA profiles for C_{10}Gua-HKUST-1 directly following synthesis (red) and after washing (blue) with EtOH at 60 °C. After washing the mass loss corresponding to organics (ligand + residual C_nGua, normalized to the guest-free formula of Cu_3BTC_2) decreases slightly indicating that some surfactant has been removed. The residual CuO at 800 °C indicates that purity has increased from 95.8 to 99% HKUST-1 following the washing procedure. The relative ease of removal strongly suggests that C_nGua is largely restricted to the crystal surface.

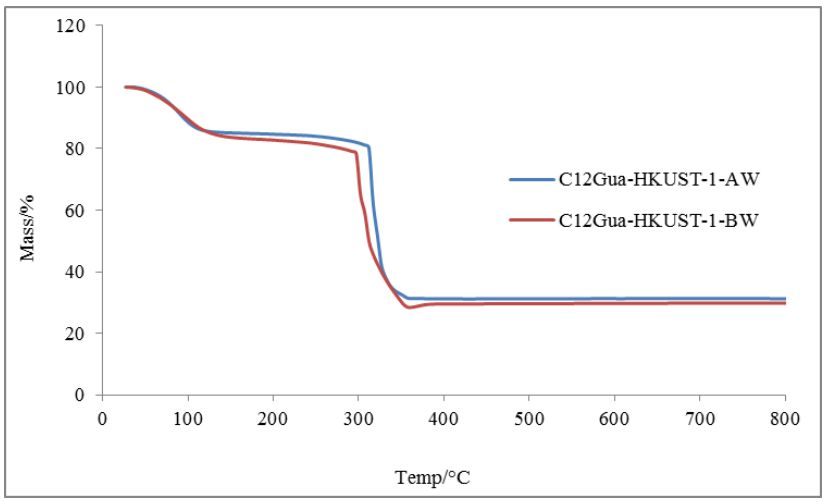

Figure S4. TGA profiles for C_{12}Gua-HKUST-1 directly following synthesis (red) and after washing (blue) with EtOH at 60 °C. After washing the mass loss corresponding to organics (ligand + residual C_nGua normalized to the guest-free formula of Cu_3BTC_2) decreases slightly indicating that some surfactant has been removed. The residual CuO at 800 °C indicates that purity has increased from 95.7 to 98.7% HKUST-1 following the washing procedure.

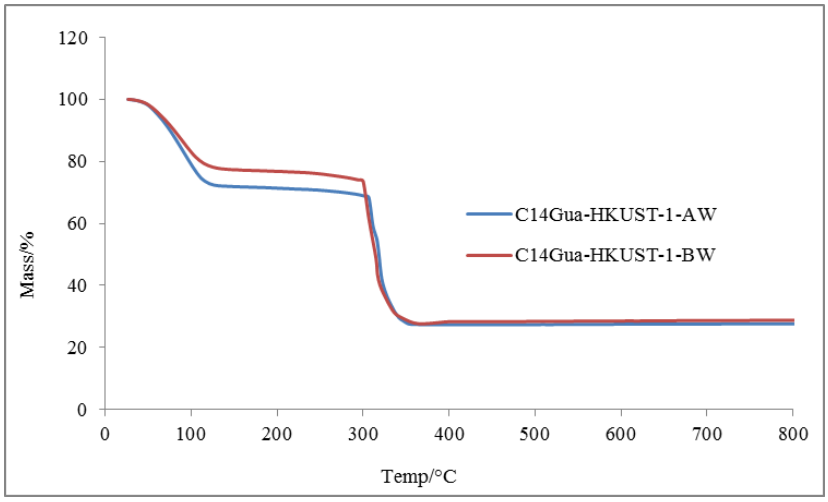

Figure S5. TGA profiles for C_{14}Gua-HKUST-1 directly following synthesis (red) and after washing (blue) with EtOH at 60 °C. In this case the residual CuO at 800 °C is identical both before and after washing, indicating that purity is > 99% HKUST-1. Minor variations between the surfactant systems arise due to slightly differing solubilities of the C_nGua species.

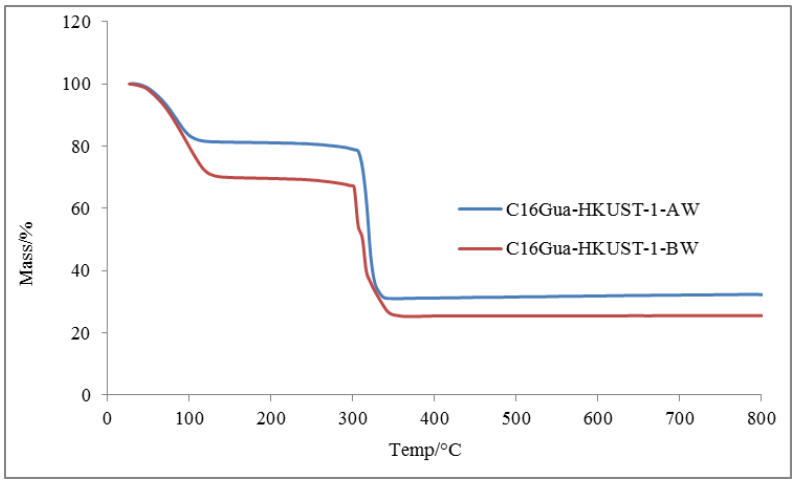

Figure S6. TGA profiles for C_{16}Gua-HKUST-1 directly following synthesis (red) and after washing (blue) with EtOH at 60 °C. After washing the mass loss corresponding to organics (ligand + residual C_nGua normalized to the guest-free formula of Cu_3BTC_2) decreases slightly indicating that some surfactant has been removed. The residual CuO at 800 °C indicates that purity has increased from 95.7 to 98.9 % HKUST-1 following the washing procedure.

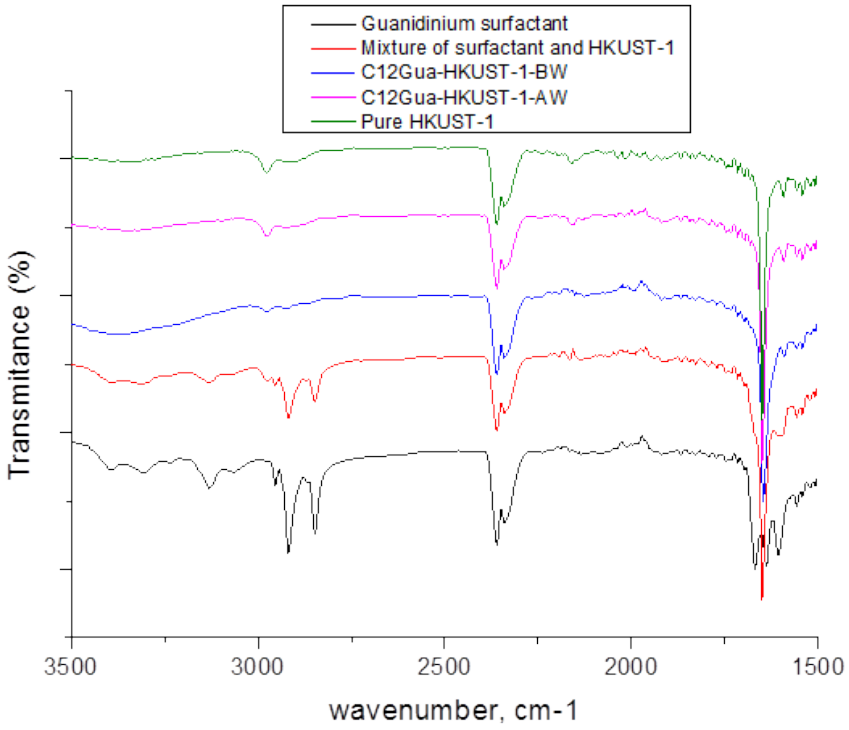

Figure S7. FTIR data of C_{12}Gua-HKUST-1 phases before/after washing (blue and cyan, respectively) compared to pure C_{12}Gua (black), HKUST-1 (green) and a physical mixture of HKUST-1 and 20 wt% C_{12}Gua (red). C_{12}Gua is not visible in the as-made or washed C_{12}Gua-HKUST-1 phases, further confirming the very low residual amount found by TGA.

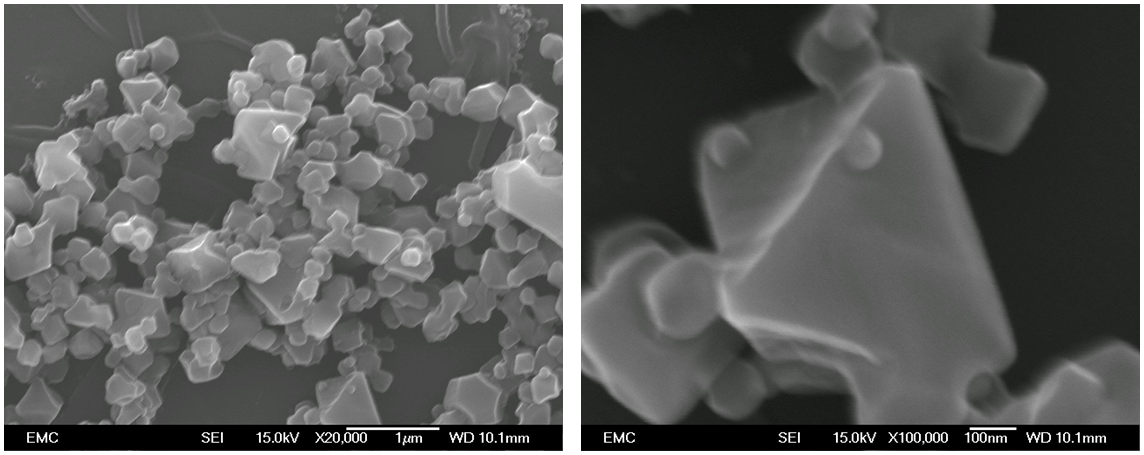

Figure S8. SEM images of C_{12}Gua-HKUST-1 as representative for C_nGua-HKUST-1 phases immediately following synthesis, which clearly show smooth featureless crystal surfaces.

Figure S9. Experimental set-up to control the moisture exposure to C_nGua-HKUST-1 phases when investigating the role of water in the etching process. (Left) samples were placed in a desiccator to provide a low humidity environment relative to the laboratory atmosphere and (right) a sealed vessel containing C_nGua-HKUST-1 and an open vial of water to increase humidity levels.

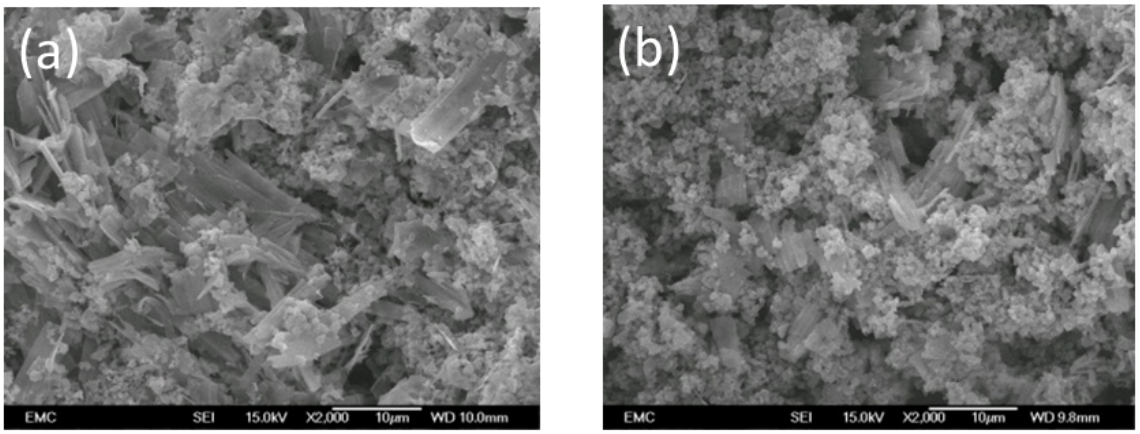

Figure S10. SEM images of (a) C_{12}Gua-HKUST-1 and (b) C_{14}Gua-HKUST-1 following exposure to a moisture rich environment.

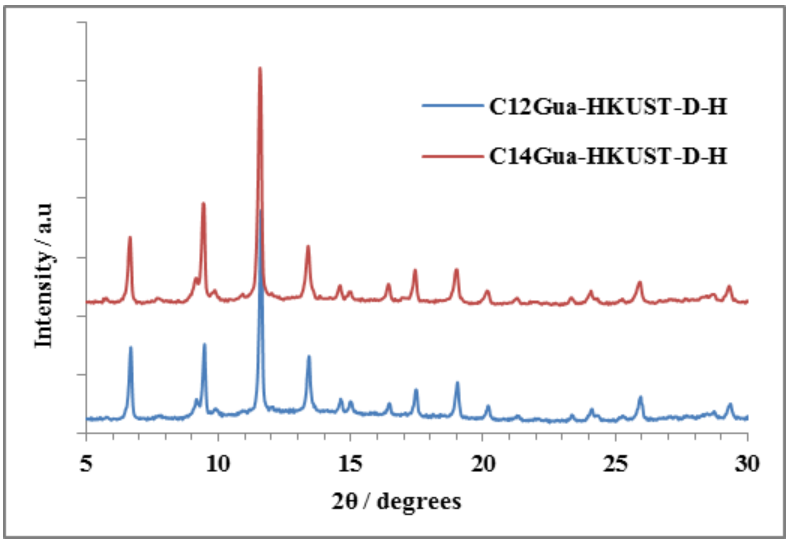

Figure S11. PXRD patterns of C_{12}Gua-HKUST-1 and C_{14}Gua-HKUST-1 following exposure to a moisture rich environment. The appearance of additional peaks and broadening of existing ones is consistent with the deterioration of the material under these conditions as highlighted in figure S9.

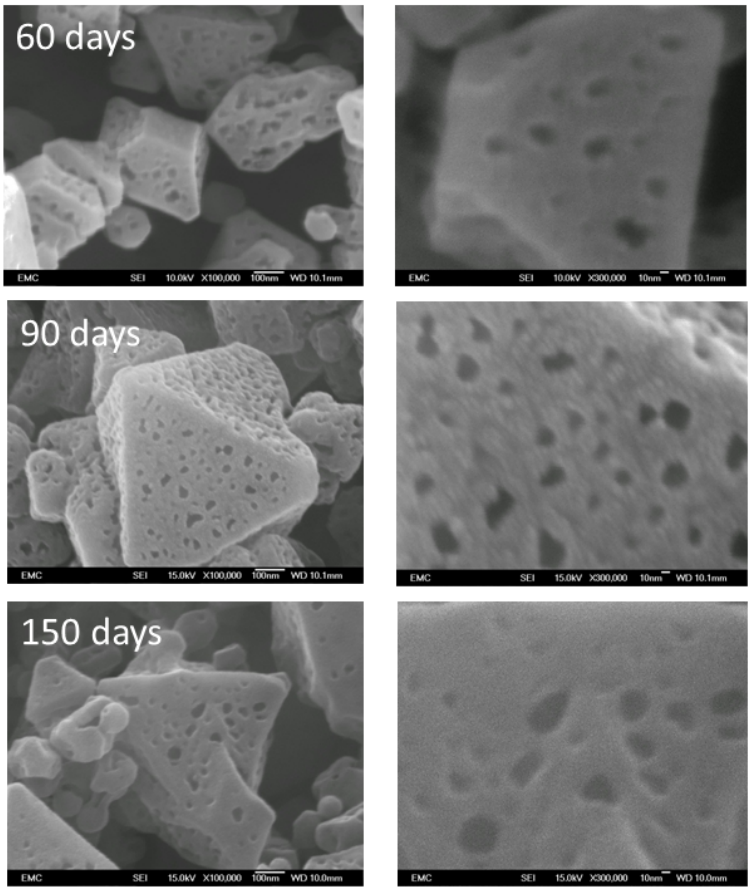

Figure S12. SEM images of C_{14}Gua-HKUST-1 following storage in a desiccator for various periods of time. Scale bars are 100 nm (left images) and 10 nm (right images).

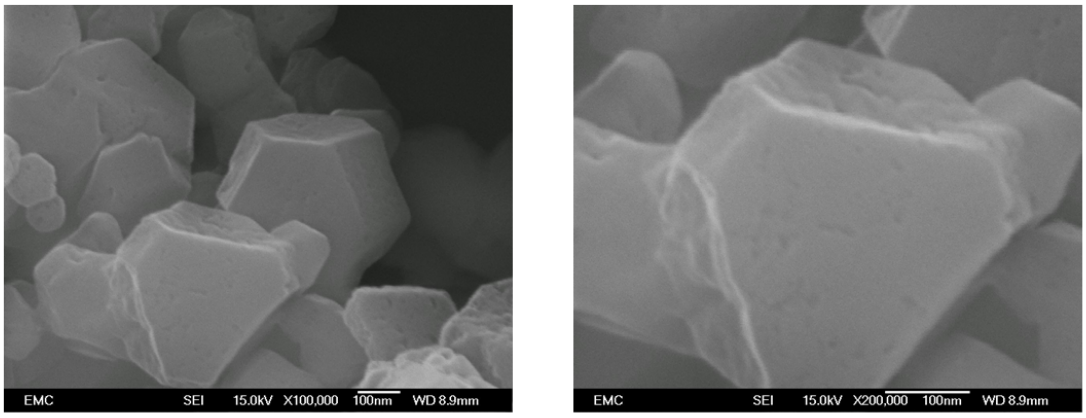

Figure S13. HKUST-1 following storage in a desiccator for 150 days.

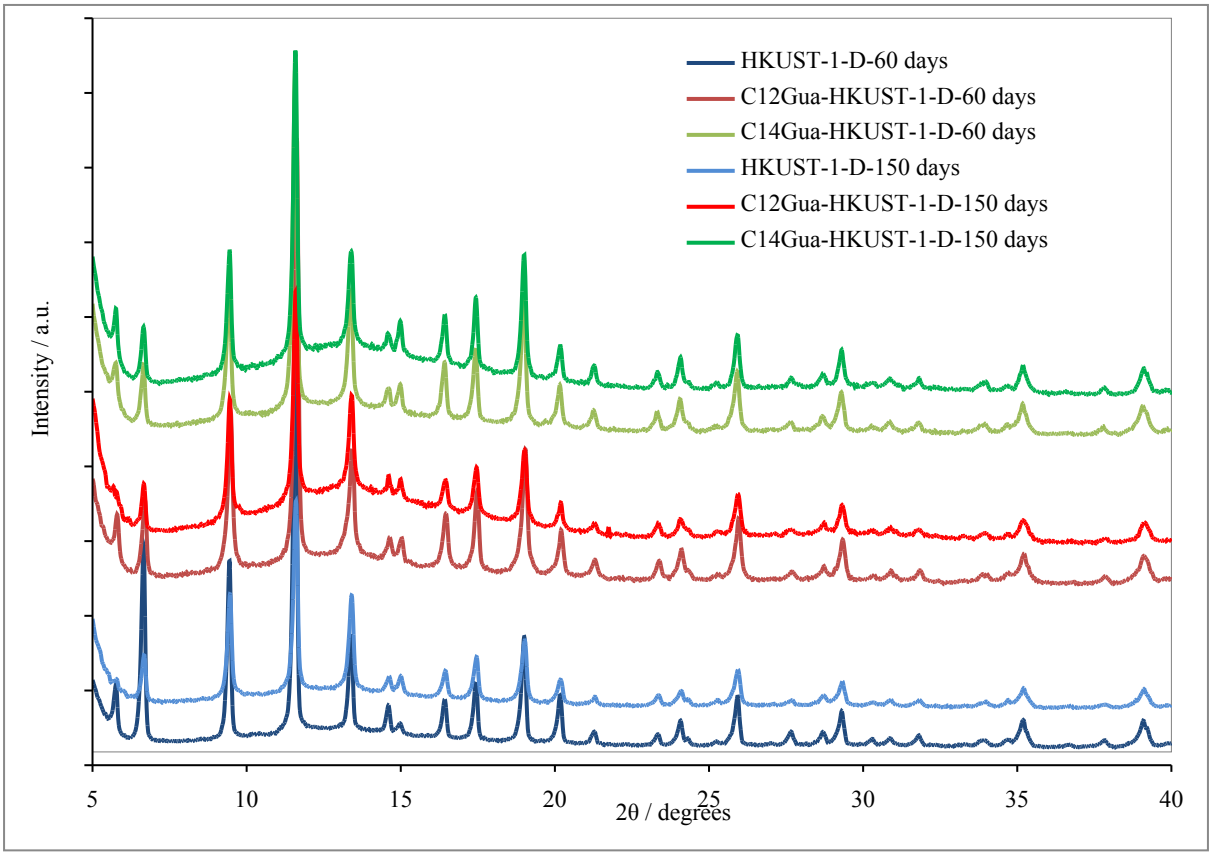

Figure S14. PXRD data of C_nGua-HKUST-1 (n = 12, 14) and pure bulk HKUST-1 following storage in a desiccator for periods of up to 150 days clearly indicating that the framework structure is intact.

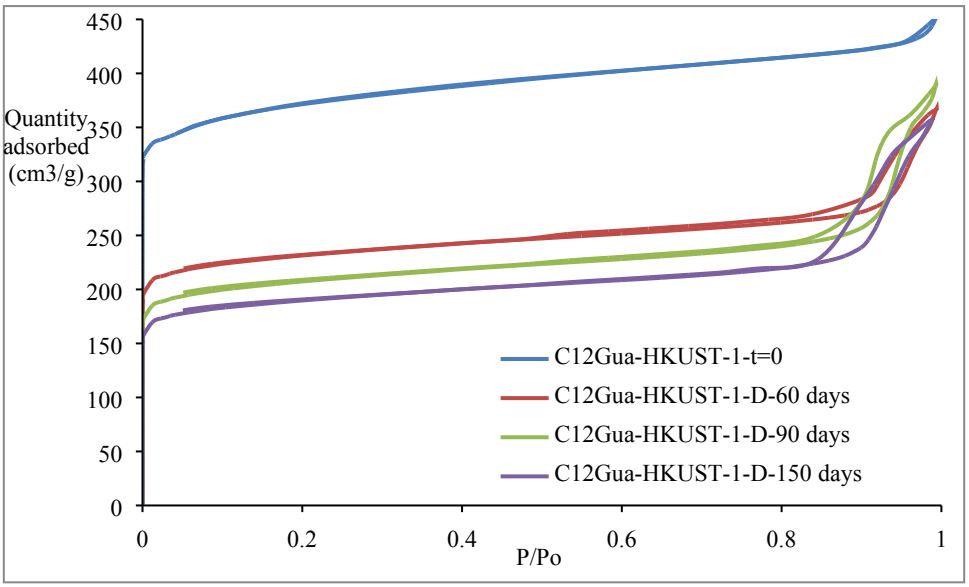

Figure S15. N_2 adsorption-desorption isotherms at 77K of C_{12}Gua-HKUST-1 following storage under low humidity conditions in a desiccator for various periods of time. The blue type I isotherm is for C_{12}Gua-HKUST-1 immediately following synthesis (t = 0), and corresponds to the smooth-faceted crystals shown in figure S8. It is clear that microporosity is reduced with increasing storage time, as also shown in table S2.

Material and storage time	**Micropore uptake[a] / cm^3g^{-1}**	**S_{BET} / m^2g^{-1}**	**Average (meso)pore diameter[b] / nm**
C_{12}Gua-HKUST-1 (as made)	383	1435	-
C_{12}Gua-HKUST-1 (60 days)	238	897	29
C_{12}Gua-HKUST-1 (90 days)	214	802	22
C_{12}Gua-HKUST-1 (150 days)	196	736	17
C_{12}Gua-HKUST-1 (60 days, then exposure)	201	774	33
C_{12}Gua-HKUST-1[c]	167	653	73

[a] Determined at p/p^0 = 0.3; [b] Estimated at the maximum of the BJH pore size distribution; [c] This sample was stored on the bench from the outset and corresponds to the C_{12}Gua-HKUST-1 entry in table S1.

Table S2. Porosity data and surface properties of C_{12}Gua-HKUST-1 phases following desiccator storage determined from the N_2 adsorption isotherms shown in figure S13.

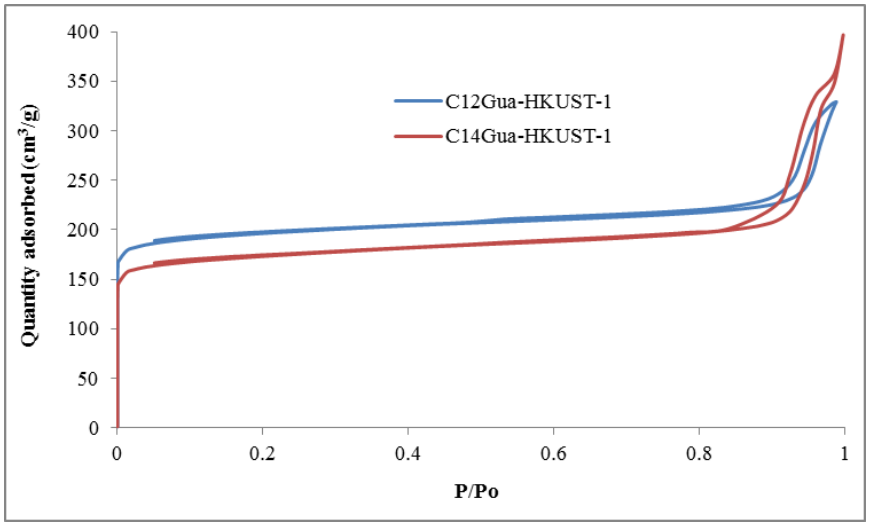

Figure S16. N_2 adsorption-desorption isotherms at 77K of C_{12}Gua-HKUST-1 and C_{14}Gua-HKUST-1 phases following exposure to the laboratory atmosphere after storing in a desiccator for two months.

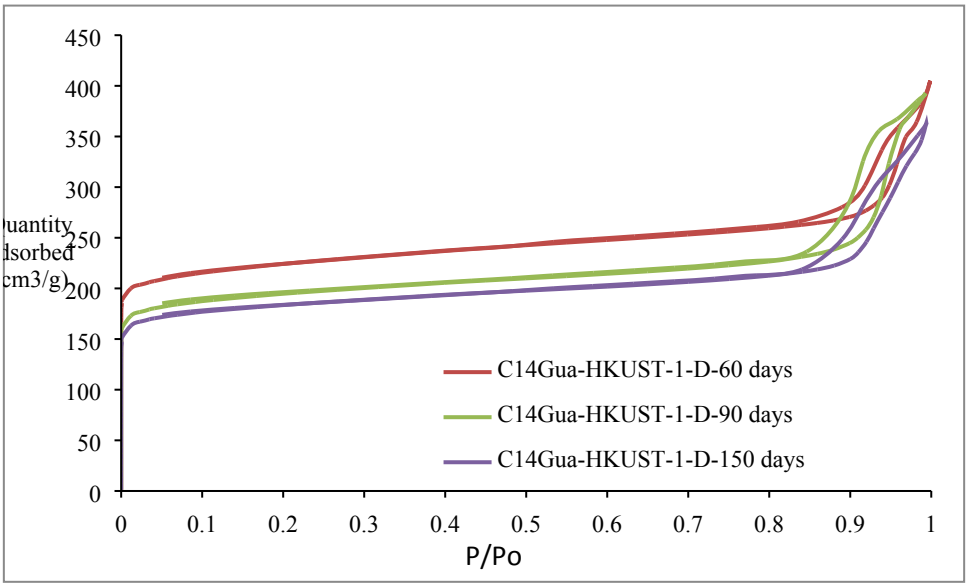

Figure S17. N_2 adsorption-desorption isotherms at 77K of C_{14}Gua-HKUST-1 following storage under low humidity conditions in a desiccator for various periods of time.

Material and storage time	Micropore uptake[a] / cm^3g^{-1}	S_{BET} / m^2g^{-1}	Average (meso)pore diameter[b] / nm
C_{14}Gua-HKUST-1 (60 days)	232	865	29
C_{14}Gua-HKUST-1 (90 days)	201	753	22
C_{14}Gua-HKUST-1 (150 days)	190	712	20
C_{14}Gua-HKUST-1 (60 days, then exposure)	178	679	32
C_{14}Gua-HKUST-1[c]	149	581	53

[a] Determined at $p/p^0 = 0.3$; [b] Estimated at the maximum of the BJH pore size distribution; [c] This sample was stored on the bench from the outset and corresponds to the C_{14}Gua-HKUST-1 entry in table S1.

Table S3. Porosity data and surface properties of C_{14}Gua-HKUST-1 phases following desiccator storage determined from the N_2 adsorption isotherms shown in figure S15.

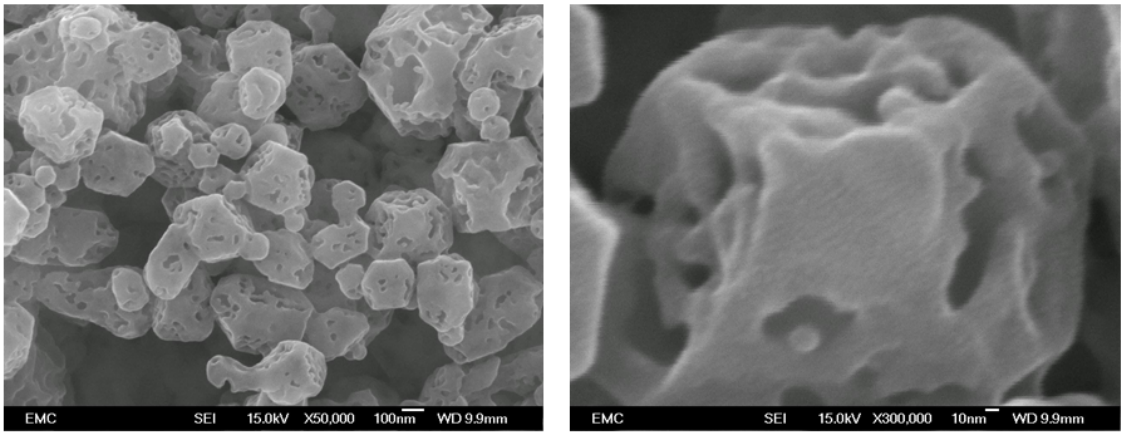

Figure S18. SEM images of C_{14}Gua-HKUST-1 after 60 days storage in a desiccator followed by exposure to the laboratory atmosphere.

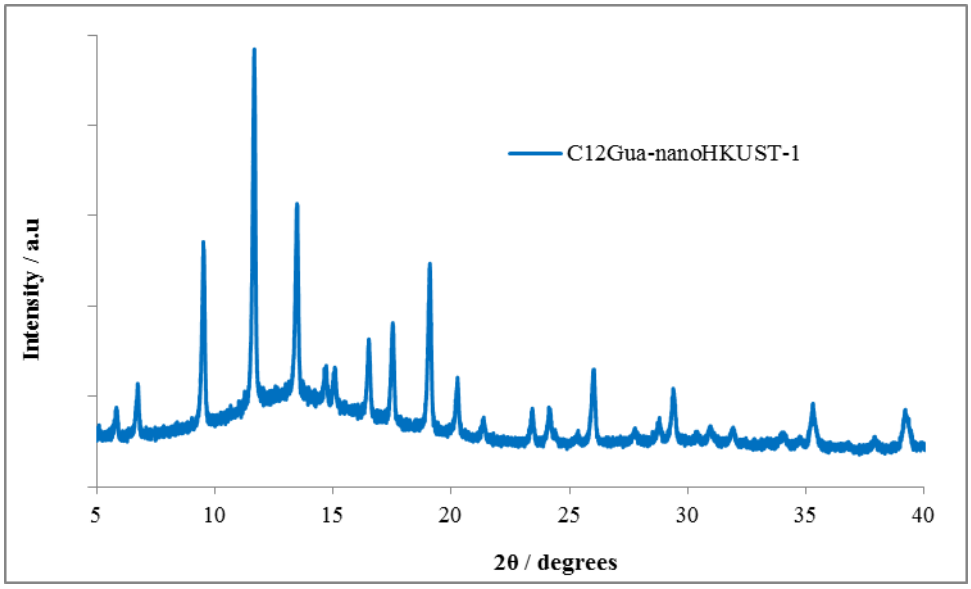

Figure S19. PXRD pattern of HKUST-1 nanoparticles prepared by following path b (C_{12}Gua + $Cu(OAc)_2$, followed by the BTC linker and solvothermal synthesis) outlined in manuscript scheme 1.

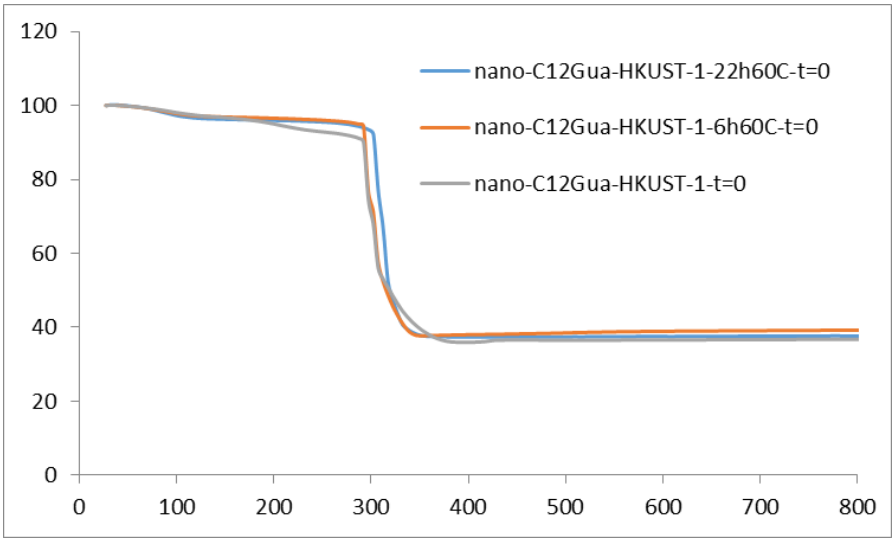

Figure S20. TGA data for HKUST-1 nanoparticles formed in the presence of a C_{12}Gua surfactant before and after washing in EtOH at various time periods. The residual mass of CuO indicates that no C_{12}Gua remains in the samples.

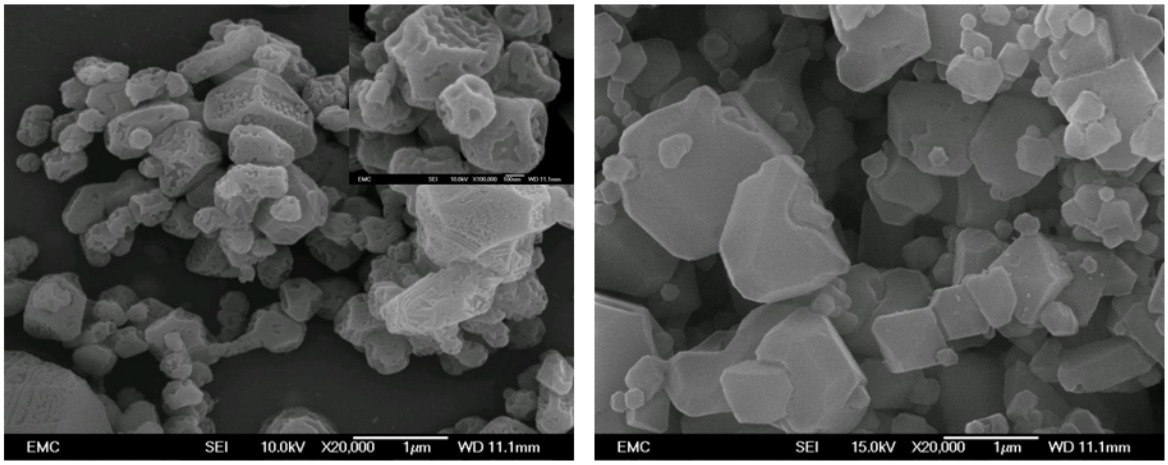

Figure S21. SEM images of C_{14}Gua-HKUST-1 (left) and pure smooth-surface HKUST-1 (right) used to pack the HPLC columns, emphasizing the similarity between particle size and distribution. Scale bars are 1 µm (100 nm for inset, left).

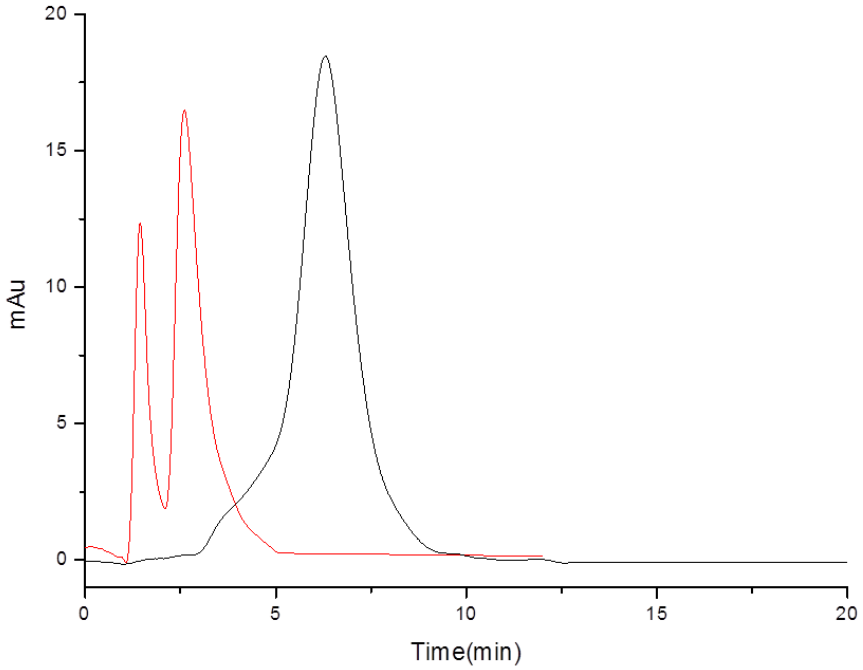

Figure S22. Comparison of columns packed with commercial Basolite C300 (black elution profile) and C_{14}Gua-HKUST-1 with meso-and macroscale surface features (red elution profile) for the HPLC separation of ethylbenzene and styrene. Ethylbenzene is eluted before styrene in both cases. Conditions: injection volume 1µL, flow rate 1 cm3 min-1, heptane:dichloromethane 98:2 v/v as the mobile phase.